Monodispersed Bioactive Glass Nanoparticles Enhance the Osteogenic Differentiation of Adipose-derived Stem Cells through ActivatingTGF-beta/Smad3 Signaling Pathway

Yi Guo [a], Yumeng Xue [a], Wen Niu [a], Mi Chen [a], Min Wang [a], Peter X Ma [a, e], Bo Lei [a, b, c, d]*

Y. Guo, Y. Xue, W. Niu, M. Chen, M. Wang, Prof. P. X. Ma, Prof. B. Lei

[a] *Frontier Institute of Science and Technology, Xi'an Jiaotong University, Xi'an 710054, China*

Prof. B. Lei

[b] *State Key Laboratory for Mechanical Behavior of Materials, Xi'an Jiaotong University, Xi'an 710054, China*

Prof. B. Lei

[c] *State Key Laboratory for Manufacturing Systems Engineering, Xi'an Jiaotong University, Xi'an 710054, China*

Prof. B. Lei

[d] *Instrument Analysis Center, Xi'an Jiaotong University, Xi'an 710054, China*

Prof.P. X. Ma

[e]Department of Biologic and Materials Sciences, Department of Biomedical Engineering, Macromolecular Science and Engineering Center, Department of Materials Science and Engineering, University of Michigan, Ann Arbor 48109, USA

* Corresponding author: Bo Lei, rayboo@xjtu.edu.cn

Abstract

The osteogenic differentiation regulation of adipose-derived stem cells (ASCs) plays a critical role in bone regeneration. It is important to understand the interaction mechanisms between nanomaterials and ASCs for biomedical application. Nanoscale bioactive glass has positive effects on guiding osteoblasts differentiation and bone regeneration. However, the effects and molecular mechanism of monodispersed bioactive glass nanoparticles (BGNs) on the osteogenic differentiation of ASCs are still not clear up to now. In this study, the effects and underlying molecular mechanism of monodispersed BGNs with different concentrations on the osteogenic differentiation of ASCs were investigated in minute detail. The results showed that BGNs (100-200 nm) could be absorbed by ASCs and was distributed in cytoplasm and nucleus. In both culture conditions (normal and osteoinductive), BGNs (80 μg/mL) could significantly enhance the osteogenic differentiation of ASCs through upregulating the ALP activity, osteogenic genes and protein expressions (*Runx2* and *Opn*), as well as calcium deposition. Further study suggested that the activation of TGF-beta/Smad3 signaling pathway plays an important role in the osteogenic differentiation of ASCs enhanced by monodispersed BGNs. This study

may have important implications for better understanding of ASCs fate induced by monodispersed BGNs and provide a promising approach toward ASCs-based bone regeneration.

Key words： Monodispersed bioactive glass nanoparticles; Adipose-derived stem cells; Osteogenic differentiation; Signaling pathway;

1. Introduction

Mesenchymal stem cells are thought to be multipotent cells, which have the ability to differentiate into multiple cell types *in vitro*, including cartilage, adipose, muscle, bone, neuron and liver. [1, 2] The cultivation and selective differentiation of mesenchymal stem cells (MSC) are important to tissue engineering. [3] And the bone marrow MSC (BMSC) has been regarded as the gold-standard of adult mesenchymal stem cells. [4] However, the harvest of bone marrow is a relatively painful procedure and the yields of stem cells are also very low (bone marrow aspirate per mL contain only 0.001 to 0.01% stem cells), which may restrict their biomedical applications. [5] To overcome these drawbacks for BMSCs, the adipose-derived stem cells (ASCs) have been proposed as an alternative stem cell population. [6] In contrast to bone marrow, 1 gram of adipose tissue includes approximately 10% ASCs and the harvest is also obtained easily. [7, 8] Owing to the self-renewal and regenerative capacity, ASCs have been induced to differentiate into desired cell types for applications in regenerative medicine and tissue engineering. [9] As such, the ASC may be a more suitable stem cell than the bone marrow MSC for clinical tissue regeneration application.

Due to the increasingly aged population and traffic accident, bone tissue engineering has drawn much attention in recent years. [10, 11] Here, ASCs play an important role in enhancing bone tissue repair and regeneration. However, how to direct the osteogenic differentiation of ASCs efficiently has become the key factor for their successful application in bone tissue engineering. [12] The osteogenic differentiation of ASCs could be induced by bioactive materials, osteogenic chemicals and growth factors. [13-15] For example, D-glyceraldehyde-3-phosphate, L-ascorbic acid, and dexamethasone have been used to induce the osteogenic differentiation of ASCs *in vitro*, however, their safety *in vivo* was still not clear. [16] The biological growth factors such as bone morphogenetic proteins (BMPs) were also employed to induce the osteogenic differentiation of ASCs, but they usually showed high cost and low specificity. [17] Bioactive biomaterials such as bioactive glass (BG) possessed inherent enhanced osteogenic differentiation ability for BMSCs and osteoblasts, as well as reinforced bone tissue regeneration *in vivo*. [18-20] However, previous studies showed that bioactive glass scaffolds have no significant effects on the osteogenic differentiation of ASCs. [21]

There are increasing pieces of evidence that nanoscale biomaterials could significantly enhance the osteogenic differentiation of MSC and tissue formation *in vivo*. [22, 23] For examples, gold nanoparticles, well-ordered $SrTiO_3$ nanotube arrays, amino acid-functionalized calcium phosphate nanoparticles could stimulate the osteogenic differentiation of MSCs. [24] Different from the macroscale bioactive glass-based biomaterials, bioactive glass nanoparticles (BGNs) possess biomimetic micro-nanoscale topological structure, high surface area, enhanced biomineralization ability and bone tissue regeneration activity. [25] Monodispersed BGNs were also developed and have shown promising applications in bioimaging, drug/gene delivery. [26, 27] Monodispersed nanoscale particle size could be easily absorbed by cells and probably induce some positive differentiation behavior of cells. Previous studies also demonstrated that BGNs could efficiently improve the osteogenic differentiation of osteoblasts and BMSCs through a MAPK pathway. [28, 29] Although the effect of nanoscale biomaterials on stem cell fate is evident, the interactions and molecular mechanisms between biocompatible nanoparticles and ASCs are still not demonstrated in detail.

Herein, the effects of monodispersed BGNs on the osteogenic differentiation of ASCs and related molecular mechanism were studied. We investigated the effects of BGNs on the proliferation, alkaline phosphatase activity (ALP), osteogenic protein and genes expressions, and calcium mineralization of ASCs. Recent studies illustrated that both the Smad and p38 MAPK pathways in TGF-beta play a critical role in *Runx2* expression and corresponded osteogenic differentiation in mesenchymal precursor cell differentiation. [30, 31] And BGNs could significantly enhance the *Runx2* expressions even under the normal growth medium. Therefore, we hypothesized that monodispersed BGNs may interact and internalize with ASCs, and activate the TGF-beta/Smad3 signaling pathway to induce ASCs osteogenic differentiation.

2. Materials and methods

2.1 Synthesis and characterization of monodispersed BGNs

The preparation process of BGNs ($80SiO_2$-$16CaO$-$4P_2O_5$) was described in our previous study. [26]The morphology was observed by transmitted electron microscope (TEM, H-8000, Hitachi). The elemental composition was measured through energy dispersive spectroscopy (EDS) analysis on the field emission scanning electron microscope (FE-SEM, SU8010, Hitachi). The Fourier transform infrared (FT-IR) spectrometer (Nicolet 6700, Thermo Scientific Instrument) was used to analyze the chemical structure of BGNs. The spectra were obtained in the range of 4000−400 cm^{-1} at a resolution 4 cm^{-1}. The specific zeta potential and hydrodynamic size were evaluated through laser particle size analyzer (Zetasizer Nano ZS, Malvern) respectively.

2.2 Cell culture and cytotoxicity analysis

Adipose tissue-derived stem cells (ASCs) were obtained from ATCC (American Type Culture Collection). The cells were cultured in (normal growth medium) Dulbecco's Modified Eagle Medium (DMEM, GIBCO) with 15% (V/V) fetal bovine serum (FBS, Invitrogen), 100U/mL penicillin and 100mg/mL streptomycin at 37 ºC in humidified air containing 5% CO_2. The BGNs were dispersed in the aseptic water and sterilized at 60 ºC in oven overnight. The ASCs were seeded onto 96-well plates at a concentration of 1500 cells per well with normal growth medium. After 24 h, the medium was changed to fresh growth medium with 60 µg/mL, 120 µg/mL and 240 µg/mL of BGNs. The medium was changed every 2 days and the cells were cultured for 1 to 5 days. The cells on tissue culture plate in normal growth medium without BGNs were used as a negative control (NC). After 1 and 5 days, the live/dead staining experiment was performed using a live/dead kit (Life Technologies) including the ethidium homodimer-1 (0.5 µM) and calcein AM (0.25 µM) (Life technologies), according to the manufacture's instruction. Then, cells were observed by an inverted fluorescence microscope (IX53, Olympus). The cell proliferation activity was analyzed by the Alamar blue® assay (Molecular Probes). Briefly, after cultured for 1, 3 and 5 days, the cells were incubated for 4 h in a medium containing 10% (v/v) Alamar Blue at 37 °C. The fluorescent intensity was measured at a 570/600 nm filter by a SpectraMax fluorescence microplate reader (Molecular Devices). The cells-free medium containing 10% Alamar Blue was used as a blank control. At least five species per sample were tested.

2.3 Cellular uptake analysis of BGNs

The cellular uptake studies of BGNs *in vitro* were determined by a confocal laser scanning microscope (CLSM, FV1200, Olympus). To observe the fluorescence of BGNs, the photoluminescent BGNs was prepared through zinc doping. The Zn-doped BGNs possess stable fluorescent properties with a green and red emission. The zinc doping does not affect the size and surface chemistry of BGNs (Table S1 in supporting information). Briefly, after sterilized by UV light, cells were seeded on the glass cover slips with a density of 8000 cells/cm^2 and incubated in the 24-well plates. After culture for 24 h in normal growth medium, the slips with seeded cells were incubated with medium containing fluorescent BGNs (100 μg/mL)for another 24 h. Then the glass slips were washed three times by PBS, fixed for 30 min with 4%paraformaldehyde solution, followed by the nucleus staining of DAPI for 20 min. Finally, the cellular uptake was observed by the CLSM.

2.4 Osteogenic differentiation evaluations of ASCs

The osteogenic differentiation of ASCs was evaluated in normal growth medium and osteoinductive medium. The osteoinductive medium consisted of growth medium with 10 nM dexamethasone, 10 mM β-glycerophosphate and 50 μg/mL L-ascorbic acid. The ASCs with a density of 2×10^4 cells/well were seeded onto 24-well plates and then treated with different concentrations of BGNs (0 μg/mL, 20 μg/mL, 50 μg/mL, 80 μg/mL) for predetermined times. The medium was changed every 2-3 days during culture period. The osteogenic differentiation of ASCs was determined through the alkaline phosphatase activity (ALP), calcium mineralization, immunofluorescence staining, quantitative real-time polymerase chain reaction (qRT-PCR) and western blot analysis. In order to investigate the osteogenic differentiation mechanism of ASCs induced by BGNs, we added the inhibitor (SB 431542) to the osteoinductive medium (5 μM) [32, 33]. The detail procedure was followed the previous description.

2.5 Alkaline phosphatase (ALP) activity and calcium deposition

The ALP activity, as an early marker of osteogenic differentiation, was assessed on days 3, 7, and 14. Briefly, at various time points, cells were rinsed with PBS solution and digested with Trypsin-EDTA (GIBCO) solution for 2 min at 37 ºC. The cells were collected into a 1.5 mL tube and washed twice with PBS solution, then, adding the lysis solution to the tubes with sufficient mixing. After 10 min standing, the mixture was centrifuged for 15 min at 12000 rpm at 4 °C. Finally, the supernatant was measured for ALP activity using a SensoLyte pNPP ALP assay kit (AnaSpec, Fremont, CA, USA), and ALP activity was normalized to the total protein content measured using the

Pierce BCA protein assay kit (Thermo Fisher Scientific) according to manufacturer instructions. The levels of ALP activity were determined from absorbance at 405 nm using a SpectraMax fluorescence microplate reader (Molecular Devices). At least three groups per sample were analyzed. The calcium deposition and extracellular-matrix mineralization of cells were tested using an alizarin red stain kit (Genmed, Quebec) according to the manufacturer instructions. In brief, the cells were cultured according to the previous description. On day 21, the cells were washed with PBS and fixed with fixative (4% paraformaldehyde) for 20 min at room temperature. Then, the cells were gently rinsed twice with PBS solution, followed by adding 200 μL alizarin for 24 h at room temperature. After that, the cells plates were washed and the photographs were captured. The relative optical intensity for each group was calculated based on the alizarin stained pictures.

2.6Immunofluorescence staining

The osteogenic differentiation protein markers including RUNX2 and OPN were determined by the immunofluorescence staining. Briefly, on day 21, the cells were washed with PBS thrice and subsequently fixed with 4%paraformaldehyde for 20 min at room temperature. The fixed cells were washed for two times with PBS, followed by incubated with 0.1% Triton for 45 min. After blocking with 1% bovine serum albumin for 30 min, cells were incubated with primary antibodies RUNX2 (1:1,000, Abcam, Cambridge, UK) or OPN(1:200, Abcam) overnight at 4°C. After washing three times with PBS, the appropriate secondary antibodies (Alexa 488, Thermo Fisher Scientific) were added and incubated for 1 h at 37 °C in the dark. Images were captured by using a fluorescence microscope (IX53, Olympus).

2.7 Quantitative real-time polymerase chain reaction (qRT-PCR) assay

After 7 and 14 days, the cells were washed twice in PBS and the ribose nucleic acid (RNA) was harvested with Tripure reagent (Roche) under the instructions. Total RNA was converted to complementary deoxyribonucleic acid (cDNA) by using a reverse transcription reagent kit (Takara). The cDNA and SYBR green Master Mix were added to each well of the array plate. The qRT-PCR was performed on the fast-real-time PCR system (Applied Biosystems 7500). All the samples were first heated from room temperature to 95 °C for 2 min, and cycled 40 times at 95 °C for 15 s, then cooled down from 95 to 60 °C for 1 min. All target gene expression results were normalized to *Gapdh*. The experiment was repeated at least four times. The relative quantification was calculated by the ΔΔCt method.

2.8 Western blotting analysis

ASCs were cultured with BGNs (80 μg/mL) for 14 days in osteoinductive medium according to the previous description. ASCs were washed three times with PBS, lysed for 30 min in ice-cold RIPA lysis buffer (20 mM Tris· HCl, pH=8.0, 150mM NaCl and 1% TritonX-100), containing protease inhibitor cocktail and phosphates inhibitor cocktail 2. After that, the mixture was centrifuged for 15 min at 12000 rpm at 4 ºC. The protein concentration was measured by using the BCA protein assay kit (Thermo Scientific) by the supernatant. Equal aliquots of protein were heated at 100 °C for 5 min in 4×sample buffer (Invitrogen). And samples of the same volume were separated on 8-12% SDS-PAGE gels (Invitrogen). The protein was transferred to polyvinylidene difluoride membranes from gels, washed once with 1×TBS-T (20 mM Tris-HCl, pH=7.5, 150 mM NaCl and 0.1% Tween), and blocked with 5% non-fat dried milk for 40 min at the room temperature. The membranes were washed two times with 1×TBS-T followed by incubation with primary antibody of anti-SMAD3 (1:1,000), phosphor-SMAD3 (1:1,000), RUNX2, OPN antibodies and GAPDH (1:1,000; Abcam) as housekeeping protein overnight at 4 °C. After two times wash with 1×TBS-T, the membranes were incubated with secondary antibody(Anti-mouse lgG, Abcam) for 60 min at the room temperature, followed by another three times wash with 1×TBS-T before protein bands visualized with ECL kit (CWBIO, Beijing, China). Finally, the membranes were taken pictures by the chemical luminescence-imaging system (Chemi Doc XRS, Bio-Rad). The relative proteins expression levels were calculated and compared by Quantity One software.

2.9 Statistical analysis

All data were shown as mean ± standard deviation. Statistical significance of difference between groups was assessed by a student's t-test. *P<0.05, **P<0.01 were considered to be statistically significant.

3. Result and discussion

3.1 Synthesis and characterizations of monodispersed BGNs

The monodispersed BGNs were successfully synthesized by a typical sol-gel process. The structure characterizations of BGNs are shown in Figure S1. The TEM images showed that BGNs possess a monodispersed spherical nanoscale size of 200-300 nm (Figure S1A). The mean hydrodynamic diameter of BGNs was about 389 nm with a Zeta potential of -12 mV (Table S1). The energy dispersive spectra (EDS) demonstrated the typical elements (Si and Ca) in BGNs (Figure S1B). The FT-IR spectra exhibited the characteristic bands of Si-O-Si at 1000-1100 cm^{-1} (Figure S1C). The amorphous structure of BGNs was confirmed by the XRD analysis (Figure S1D). The synthesized monodispersed BGNs may have positive effect on the proliferation and osteogenic differentiation of ASCs.

3.2 Cellular toxicity and cell uptake of BGNs

ASCs were used to analyze the cytotoxicity of BGNs. After incubating with BGNs (0-240 μg/mL) for 1 and 5 days, no dead cells (red) were observed, which suggested the low cytotoxicity of BGNs (Figure 1A). The ASCs viability in various groups was significantly increased with the incubation time (from 1 to 5 days), indicating that BGNs with different concentrations could support the cell proliferation (Figure 1B). On day 1, the BGNs group with 60 μg/mL showed the significantly high cell viability compared with other groups (Figure 1B). On day 5, the cell viability was slightly decreased as increasing the particles concentrations. These results suggested that BGNs with the concentrations below 100 μg/mL may be suitable to investigate their effect on the osteogenic differentiation of ASCs.

Previous studies have shown that the cellular uptake of monodispersed nanoparticles probably enhanced the osteogenic differentiation of marrow stem cells (MSCs) through mechanical-responsive signal pathway. [34] Therefore, here we investigated the cellular uptake of BGNs in ASCs (Figure 2). After incubation with fluorescent BGNs (100 μg/mL) for 24 h, the bright green and red fluorescence from nanoparticles in ASCs could be observed. The CLSM images with high magnification further showed that the nanoparticles were distributed in cytoplasm and nucleus, suggesting the efficient uptake by ASCs. The intracellular distribution of BGNs may have important effect on the osteogenic differentiation of ASCs through the interaction between nanoparticles and intracellular proteins.

3.3 Osteogenic differentiation of ASCs

The osteogenic differentiation of pluripotent progenitor ASCs is a crucial step in osteogenesis. The ALP activity is an early phenotypic marker for osteogenic differentiation, and mineralized nodule formation is a phenotypic marker for last stage in mature osteoblasts. Figure 3 shows the effect of BGNs with different concentrations on the ALP activity of ASCs under normal and osteoinductive conditions (Figures 3). Under normal medium condition, the ALP activity of ASCs was increased significantly with the BGNs concentration (Figure 3A). Compared with other groups, BGNs at 80 μg/mL showed the significantly high ALP activity on day 7. Different from the normal condition, the ASCs in BGNs 80 μg/mL also have exhibited the highest ALP activity on day 7, among all groups (Figure 3B). The results showed that BGNs with suitable concentration could significantly enhance the ALP activity of ASCs. In addition, the Alizarin Red staining evaluation showed that BGNs could significantly improve the calcium mineralization of ASCs after 21 days (Figure 4). Under normal and osteoinductive condition, BGNs groups with various concentrations demonstrated the significantly high positive staining compared with tissue culture plate (NC) (Figure 4A). The relative intensity calculation further confirmed that BGNs groups have the significantly high positive staining either normal or osteoinductive condition (Figures 4B-C). These results suggested that BGNs could significantly enhance the calcium deposition and mineralization of ASCs.

The immunofluorescence staining for RUNX2and OPN proteins in ASCs on day 21 is shown in Figures 5. Under normal medium condition, there was no obvious positive RUNX2 and OPN staining (green) in NC group (Figures 5A-B). However, as the addition of BGNs, the significant positive protein staining was observed (Figures 5A-B). BGNs with 80 μg/mL showed observably higher fluorescence intensity associated with RUNX2 and OPN expression as compared with other groups (Figures 5C, E). Under osteoinductive condition, the RUNX2 and OPN protein expression showed a similar tendency with that under normal condition (Figures 5D, F). The group of 80 μg/mL BGN also showed remarkably higher fluorescence intensity associated with RUNX2 and OPN expression as compared to other groups (Figures 5). These results indicated that the appropriate concentration of BGNs could significantly enhance the osteogenic proteins expression in ASCs.

To demonstrate the effect of the uptake of BGN with different concentrations on the ASCs osteogenic differentiation at the mRNA level, we investigated the expression of osteoblastic marker genes (early-stage markers: *Runx2*; late-stage marker: *Opn)* after culture for 7 and 14 days. All marker genes expression in all groups significantly increased from day 7 to day 14 under different incubation conditions. In normal medium, as compared with other groups, the *Runx2* expression on day 7 was significantly upregulated after incubation with BGNs at 80 μg/mL (Figure 6A). On day 14, no significant difference of *Runx2* expression among various groups was observed. For *Opn* expression, on day 7 and day 14, BGNs group with 80 μg/mL showed the significantly high *Opn* level, as compared to NC and other BGNs groups (Figure 6B). In osteoinductive medium, on day 7 and 14, *Runx2* and *Opn* expression in the BGNs group with optimized concentration was significantly high as compared with the NC group (Figures 6C-D). The ALP activity, Alizarin Red staining, immunofluorescence staining and osteogenic genes analysis further demonstrated that BGNs with appropriate concentration could efficiently enhance the osteogenic differentiation of ASCs under the normal and osteoinductive conditions.

3.4 Signal pathway and molecular mechanism investigation

The molecular mechanisms of the osteogenic differentiation for stem cells induced by monodispersed bioactive glass nanoparticles are still not clear. It was shown that several signaling pathways such as BMP (bone morphogentic proteins-2)-Smads 1/5/8, TGF(transforming growth factor)-beta-Smads 2/3/4, Wnt (wingless- type)-beta-catenin,mitogen-activated protein kinases (MAPK)/extracellular regulated protein kinases (ERK) are responsible for regulating stem cells osteogenic differentiation and bone formation [35, 36] Previous studies showed that bioactive micro/nanoscale surface and nanoparticles enhanced the osteogenic differentiation of MSCs through the activation of p38 MAPK, AKT/Protein Kinase B and ERK signaling pathways. [37] However, the TGF-beta/Smad3 signaling pathway in the osteogenic differentiation of ASCs cells induced by monodispersed BGNs was not studied. Herein, it was hypothesized that BGNs probably activate the Smad3 activity, promoted the Smad3 complex into the nucleus and up-regulated the expression of osteogenic target genes. In order to detect the hypothesis, we used inhibitor (SB 431542) to inhibit the TGF-beta type I receptors (TGF-betaR I) and then Smad3 cannot be phosphorylated, which resulted in the suppression of osteogenic marker genes. As shown in Figure 7, the uptake of BGNs significantly enhanced the expressions of osteogenic RUNX2 and OPN proteins, SMAD3 and phosphorylated SMAD3 (p-SMAD3). However, after adding inhibitor (SB 431542), the RUNX2, OPN, SMAD3, p-SMAD3 protein levels were also decreased significantly (Figures 7A-E). Additionally, the mRNA expression levels of *Runx2* and *Opn* were also reduced significantly, as compared to those before adding inhibitor (Figures 7F-G). These results further demonstrated that the TGF-beta/Smad3 signaling pathway plays a critical role in the effect of monodispersed BGNs on enhancing the osteogenic differentiation of ASCs. The monodispersed BGNs probably were uptaken by ASCs via endocytosis, activated the TGF-beta/Smad3 signaling pathway, enhanced the expression of osteogenic genes and proteins, and improved the osteogenic differentiation of ASCs (Scheme 1).

Previous reports have shown that monodispersed nanoparticles have different osteogenic differentiation mechanism for stem cells, as compared to the bulk materials, because nanoparticles could enter cells and may have interaction with intracellular proteins. [44] Gold nanoparticles promote the osteogenic differentiation of BMSCs through p38 MAPK signaling pathway and human ASCs via

Wnt-beta-catenin pathway. [24, 38] Iron oxide nanoparticles could also promote osteogenic differentiation of BMSCs via MAPK pathway. [31] The silica@Ru nanoparticles also showed that they could activate the Akt pathway to enhance the osteogenic differentiation of BMSCs. [39] Nanoscale bioactive glass could improve the osteogenesis of MG-63 cells through the activation of MAPK/ERK signaling pathway. [29] Chang group also observed that hydroxyapatite scaffolds with nanoscale structure could enhance the osteogenesis of ASCs through Akt pathway. [40] Xiao and Wu group reported that silicate ions could enhance the osteogenic differentiation of BMSCs through the activation of Wnt pathway. [41] In this study, we provide a new possible TGF-beta-Smads3 signaling pathway for the osteogenic differentiation of ASCs enhanced by monodispersed BGNs. TGF-beta signaling has shown that they could enhance osteogenic differentiation via the activation of MAPKs and Smad2/3 pathways. [42] Recent studies also confirmed that the Smad pathways converge at *Runx2* gene to regulate the differentiation of mesenchymal cells. [43] Here, through inhibiting theTGF-beta type I receptor, the SMAD3, RUNX2, OPN and p-SMAD3 protein expressions were significantly decreased. The results suggested that the addition of BGNs could efficiently activate the TGF-beta/Smad3 signaling pathway and enhance the osteogenic differentiation of ASCs. However, further *in vivo* study should be necessary to demonstrate the role of BGNs on regulating ASCs differentiation and bone regeneration.

4. Conclusion

In summary, monodispersed BGNs could be uptaken by ASCs and distributed in cytoplasm/nucleus. The internalized BGNs significantly enhanced the osteogenic differentiation of ASCs through improving their ALP activity, calcium mineralization, osteogenic proteins and genes expressions, either normal or inductive conditions. We demonstrated that monodispersed BGNs can activate the TGF-beta signaling pathway through upregulating the level of p-SMAD3 protein, which efficiently facilitates the osteogenic differentiation of ASCs. This study suggests that monodispersed BGNs have great potential for ASCs-based bone tissue regeneration.

Acknowledgements

We acknowledge the valuable comments of potential reviewers. This work was supported by China Postdoctoral Science Foundation (Grant No. 2017M613148), State Key Laboratory for Mechanical Behavior of Materials (No 20161801), the Natural Science Basic Research Plan in Shaanxi Province of China (Grant No. 2015JQ5165), National Natural Science Foundation of China (Grant No. 51502237).

References

[1] Williams AR, Hare JM. Circ. Res. **2011**, 109, 923.

[2] Uccelli A, Laroni A, Freedman MS. Lancet Neurol. **2011**, 10, 649.

[3] Hwang NS, Zhang C, Hwang YS, Varghese S. Wires Syst. Biol. Med. **2009**, 1, 97.

[4] Yu M, Lei B, Gao CB, Yan J, Ma PX. Nano Research, **2017**, 10, 49.

[5] Pittenger MF, Mackay AM, Beck SC, Jaiswal RK, Douglas R, Mosca JD, Mosca, Mark A. Moorman, Donald W. Simonetti, Stewart Craig , Daniel R. Marshak. Science **1999**, 284, 143.

[6] Mizuno H, Tobita M, Uysal AC. Stem Cells **2012**, 30, 804.

[7] Oedayrajsingh-Varma MJ, Van Ham SM, Knippenberg M, Helder MN, Klein-Nulend J, Schouten TE, Mjpf Ritt & Fj van Milligen. Cytotherapy **2006**, 8, 166.

[8] Zhu YX, Liu TQ, Song KD, Fan XB, Ma XH, Cu ZF. Cell Biochem. Funct. **2008**, 26, 664.

[9] Russo V, Yu C, Belliveau P, Hamilton A, Flynn LE. Stem Cell Transl. Med. **2014**, 3, 206.

[10] Henkel J, Woodruff MA, Epari DR, Steck R, Glatt V, Dickinson IC, Choong PF, Schuetz MA Hutmacher DW. Bone Res. **2013**, 1, 216.

[11] Woodruff MA, Lange C, Reichert J, Berner A, Chen FL, Fratzl P, an-Thorsten Schantz, Dietmar W. Hutmacher. Mater. Today **2012**, 15, 430.

[12] Santo VE, Duarte ARC, Popa EG, Gomes ME, Mano JF, Reis RL. J. Control Release **2012**, 162, 19.

[13] Gonzalez-Cruz RD, Fonseca VC, Darling EM. P. Natl. Acad. Sci. USA **2012**, 109, 1523.

[14] Ravichandran R, Venugopal JR, Sundarrajan S, Mukherjee S, Ramakrishna S. Biomaterials **2012**, 33, 846.

[15] Banks JM, Mozdzen LC, Harley BAC, Bailey RC. Biomaterials **2014**, 35, 8951.

[16] Langenbach F, Handschel J. Stem Cell Res. Ther. **2013**, 4, 117.

[17] Zhou XJ, Feng W, Qiu KX, Chen L, Wang WZ, Nie W, Mo X, He C. ACS Appl. Mater. Inter. **2015**, 7, 15777.

[18] Lei B, Chen XF, Han X, Li ZM. J. Mater. Chem. **2011**, 21, 12725.

[19] Lei B, Chen XF, Han X, Zhou JA. J. Mater. Chem. **2012**,22, 16906.

[20] Xue YM, Guo Y, Yu M, Wang M, Ma PX, Lei B. Adv. Healthc. Mater. **2017**,6, 1700630.

[21] Haimi S, Gorianc G, Moimas L, Lindroos B, Huhtala H, Raty S, Hannu Kuokkanen, George K.Sándor, Chiara Schmid, Susanna Miettinen,Riitta Suuronen. Acta Biomater. **2009**, 5, 3122.

[22] Dobbenga S, Fratila-Apachitei LE, Zadpoor AA. Acta Biomater. **2016**,46, 3.

[23] Du YZ, Ge J, Li YN, Ma PX, Lei B. Biomaterials, **2018**, 157, 40.

[24] Yi CQ, Liu DD, Fong CC, Zhang JC, Yang MS. ACS Nano **2010**, 4, 6439.

[25] Isaac J, Nohra J, Lao J, Jallot E, Nedelec JM, Berdal A, Sautier JM. Eur. Cells Mater. **2011**, 21,130.

[26] Xue YM, Du YZ, Yan J, Liu ZQ, Ma PX, Chen XF, Lei B. J. Mater. Chem. B **2015**, 3, 3831.

[27] Yu M, Xue YM, Ma PX, Mao C, Lei B. ACS Appl. Mater. Inter. **2017**, 9, 8460.

[28] Gong WY, Dong YM, Chen XF, Karabucak B. Chin. J. Dent. Res. **2012**, 15, 145.

[29] Gong WY, Dong YM, Wang SN, Gao XJ, Chen XF. RSC Adv. **2017**, 7, 13760.

[30] Guo X, Liao J, Park H, Saraf A, Raphael RM, Tabata Y, F.K. Kasper, A.G. Mikos. Acta Biomater. **2010**, 6, 2920.

[31] Wang QW, Chen B, Cao M, Sun JF, Wu H, Zhao P, Xing J, Yang Y, Zhang XQ, Ji M, Gu N. Biomaterials **2016**, 86, 11.

[32] Quarto N, Li SL, Renda A, Longaker MT. Stem Cells **2012**, 30, 2709.

[33] Koli K, Ryynanen MJ, Keski-Oja J. Bone **2008**, 43, 679.

[34] Li JC, Chen Y, Yang YJ, Kawazoe N, Chen GP. J. Mater. Chem. B **2017**, 5, 1353.

[35] Ng F, Boucher S, Koh S, Sastry KSR, Chase L, Lakshmipathy U, Cleo Choong, Zheng Y, Mohan C. Vemuri, Mahendra S. Rao, Vivek Tanavde. Blood **2008**, 112, 295.

[36] Su X, Liao L, Shuai Y, Jing H, Liu S, Zhou H, Y Liu, Y Jin. Cell Death Dis. **2015**, 6, 221.

[37] Jiao K, Niu LN, Li QH, Chen FM, Zhao W, Li JJ, Chen JH, Christopher W.Cutler, David H.Pashley, Franklin R.Tay. Acta Biomater. **2015**, 19, 23.

[38] Choi SY, Song MS, Ryu PD, Lam ATN, Joo SW, Lee SY. Int. J. Nanomed. **2015**, 10, 4383.

[39] Liu Y, Huang N, Yu YF, Zheng CP, Deng N, Liu J. J. Mater. Chem. B **2016**, 4, 4389.

[40] Xia LG, Lin KL, Jiang XQ, Fang B, Xu YJ, Liu JQ, Zeng DL, Zhang ML, Zhang XL, Chang J, Zhang ZY. Biomaterials **2014**, 35, 8514.

[41] Han PP, Wu CT, Xiao Y. Biomater. SCI-UK **2013**, 1, 379.

[42] Rhyu DY, Yang YQ, Ha HJ, Lee GT, Song JS, Uh ST, Lee HB. J. Am. Soc. Nephrol. **2005**, 16, 667.

[43] Lee KS, Hong SH, Bae SC. Oncogene **2002**, 21, 7156.

[44] Yang KN, Cao WP, Hao XH, Xue X, Zhao J, Liu J, Zhao YL, Meng J, Sun BY, Zhang JC, Liang XJ. Nanoscale **2013**, 3, 1205.

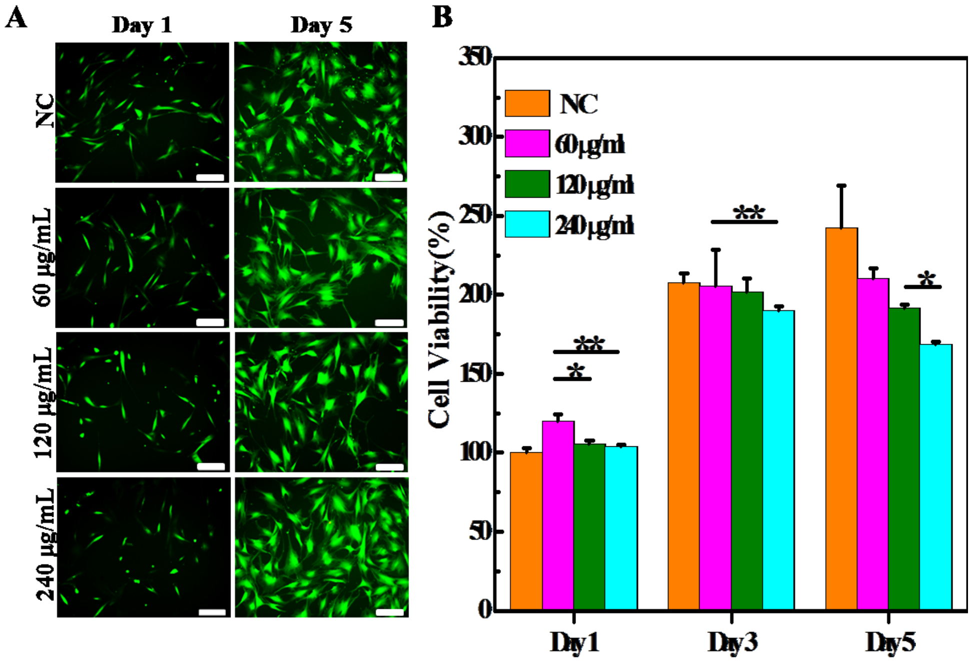

Figure 1

Figure 1. Cellular biocompatibility evaluation of ASCs following incubation with various concentration of BGNs. (A) Fluorescence images indicating live-dead staining after day 1 and 5 incubation (scale bar: 100 μm). (B) Cell viability and proliferation after culture for 1 to 5 days. **P*< 0.05 and ***P*< 0.01.

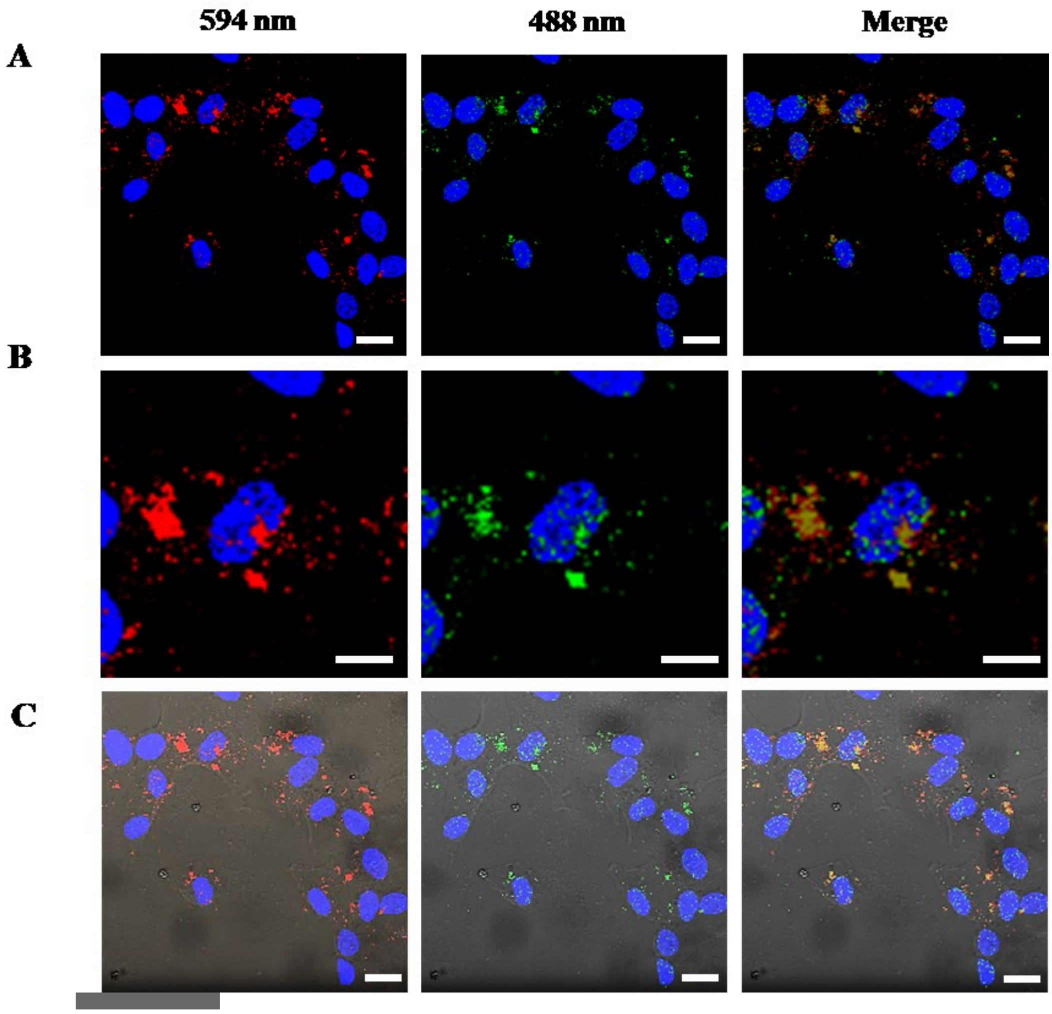

Figure 2

Figure 2. Confocal images of live ASCs cells after stained by fluorescent BGNs, the cell nuclei were stained as blue.(A) Fluorescent images of cells after excitation at 594 nm (Red) and 488 nm(Green); (B) Magnified fluorescent images ofsinglecell showing the BGNs distribution; (C) Merged images of fluorescent and bright field. Scale bar=20µm.

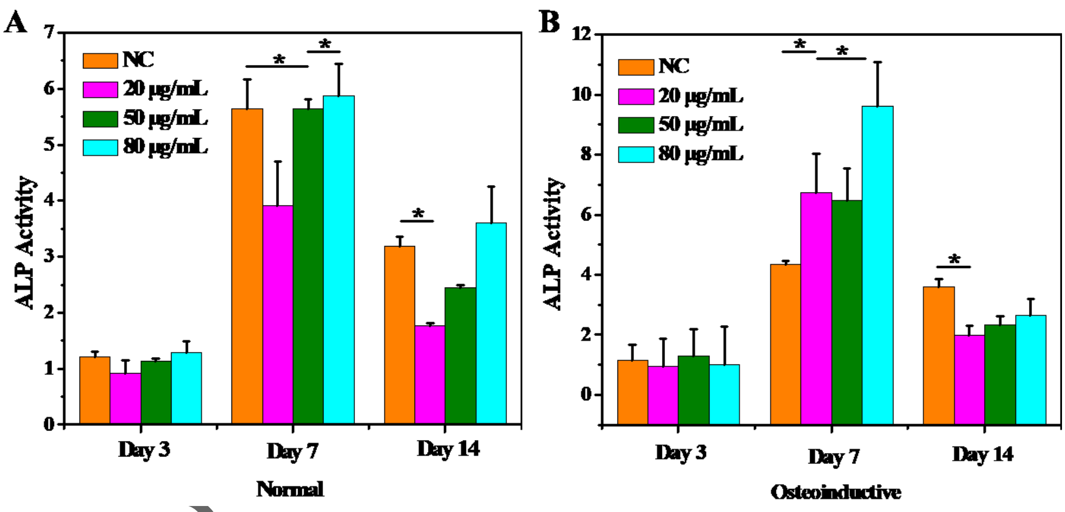

Figure 3

Figure 3. ***In vitro*** **ALP activity evaluation of ASCs following induction by various concentration of BGNs in normal and osteoinductive medium.** (A) ALP activity on days 3, 7 and 14 with normal culture medium; (B) ALP activity on days 3, 7 and 14 with osteoinductivemedium. **P*<0.05 and ***P*<0.01.

Figure 4. Calcium depositionbiomineralization staining evaluation of ASCs after incubated with various concentrations of BGNs in normal and osteoinductive medium for 21 days. (A) Alizarin red staining analysis demonstrating the effect of BGNs on mineralized nodule of ASCs; (B) The relative gray intensity based on the images of Alizarin red staining imagesanalyzed by image J. Tissue culture plate (NC) is the negative control. *P<0.05 and **P<0.01.

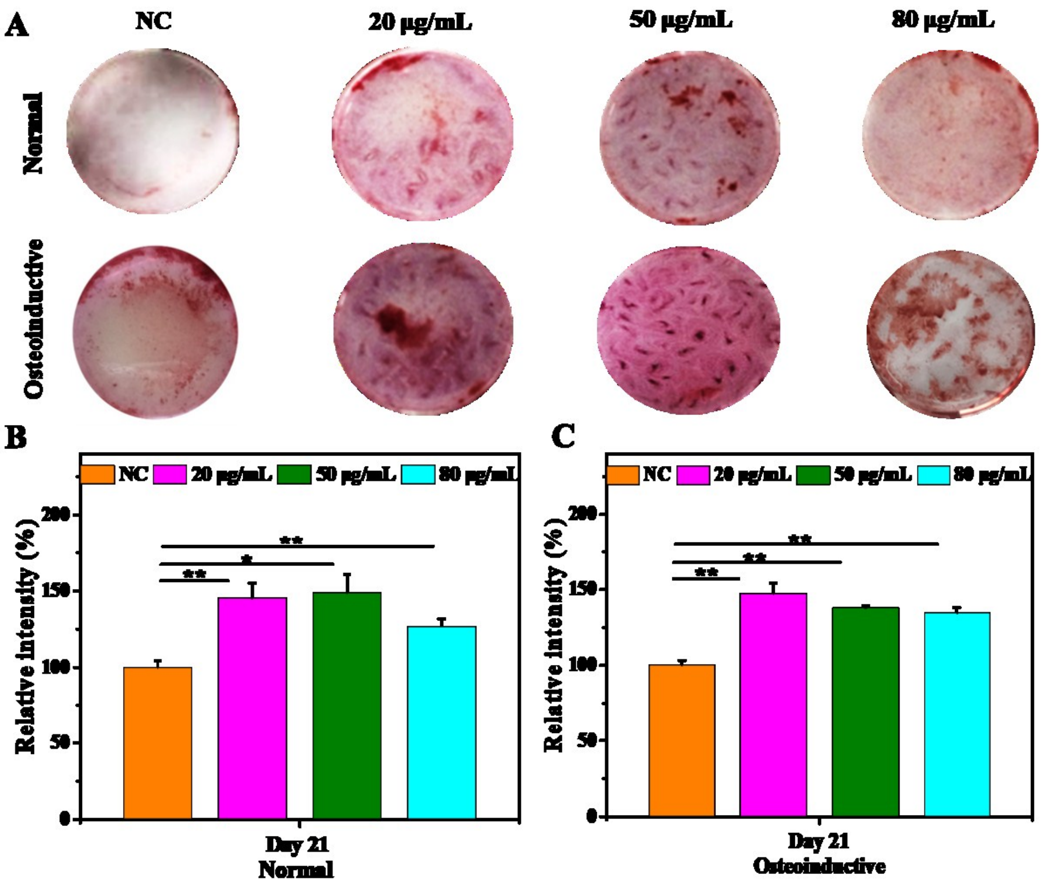

Figure 4

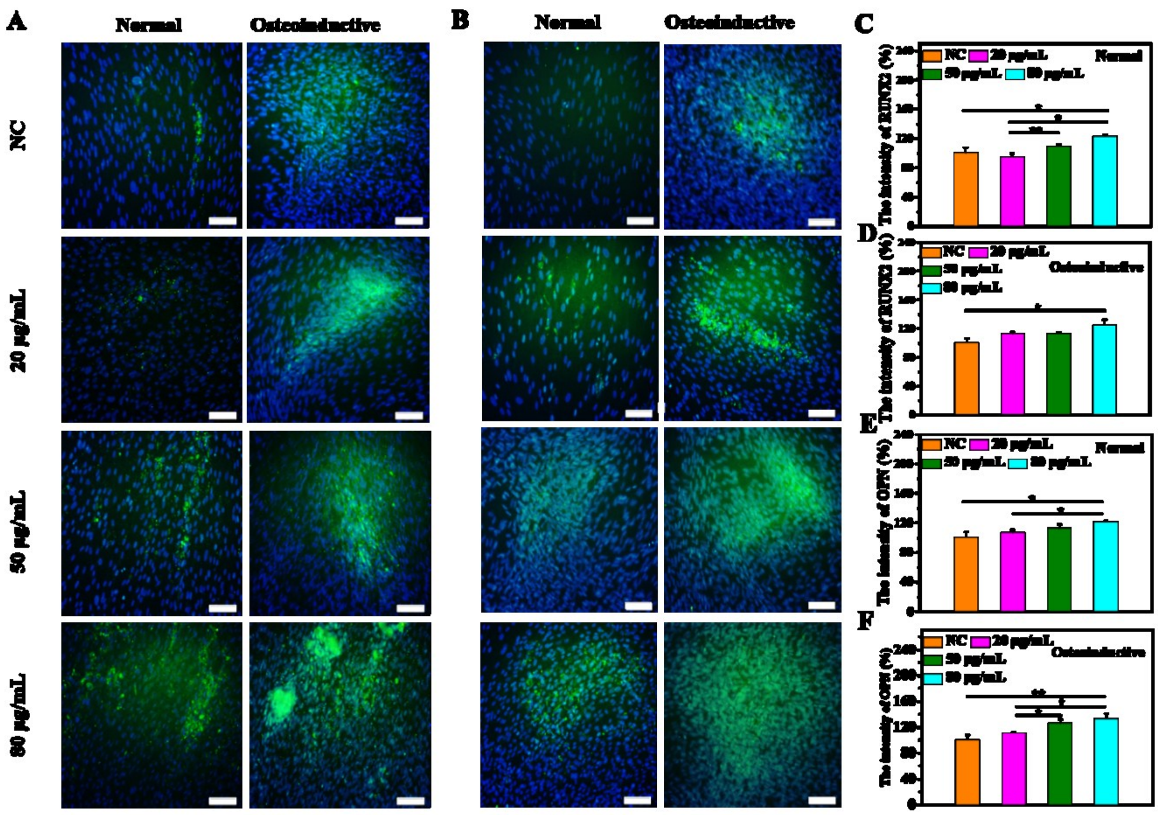

Figure 5. Immunofluorescent staining of osteogenic proteins RUNX2 and OPNin ASCs after incubated with various concentrations of BGNs in normal and osteoinductive medium for 21 days. RUNX2 and OPN areshown as green and nuclei are stained as blue. (A) Immunofluorescent staining for RUNX2protein (scale bar=in 100 μm);(B)Immunofluorescent staining of OPN protein (scale bar=in 100 μm); (C-D) Relative fluorescent intensity of RUNX2 protein under normal (C) and osteoinductive medium (D); (E-F) Relative fluorescent intensity of OPN protein under normal (E) and osteoinductive medium (F).*P<0.05 and **P<0.01. Tissue culture plate (NC) is the negative control. The relative fluorescent intensity of immunofluorescent staining was analyzed by image J based on the images.

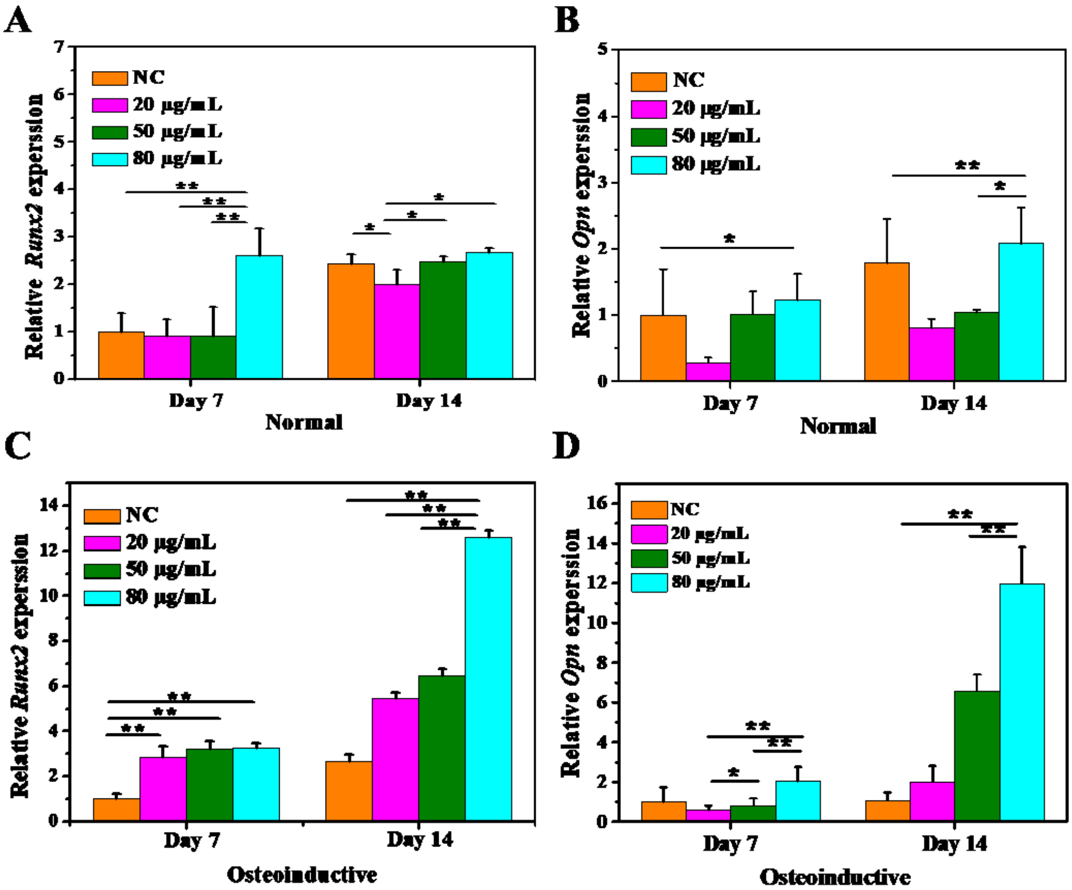

Figure 6

Figure 6. Relative expression of osteogenic marker genes of ASCs after cultured on normal and osteoinductive medium with the different concentration of BGNs for 7 and 14 days. (A-B) Relative expression of *Runx2*(A) and *Opn*(B) in normalmedium; (C-D)Relative expression of *Runx2* (C) and *Opn* (D) in osteoinductive medium.NC is the negative control. *P<0.05 and **P<0.01.

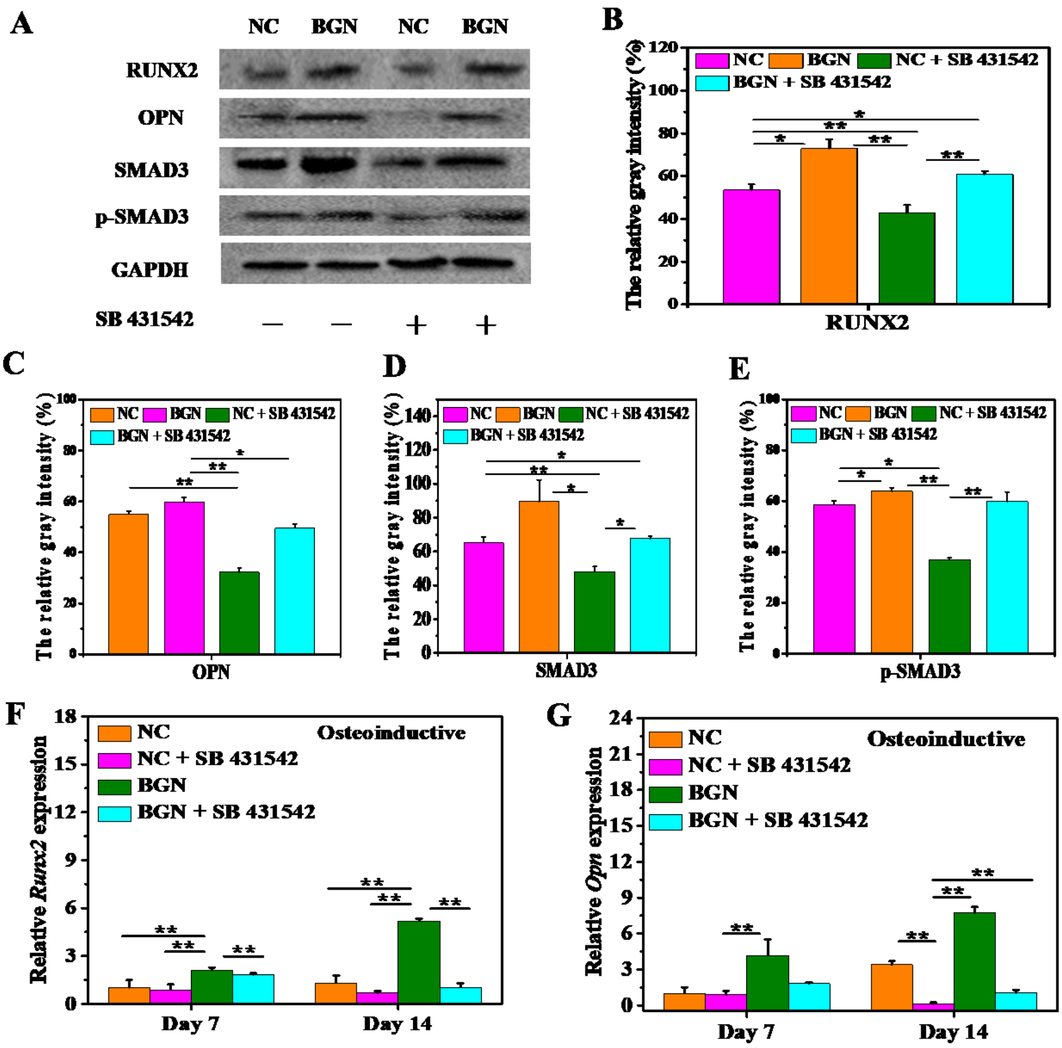

Figure 7

Figure 7. Osteogenic differentiation mechanism investigation of ASCs induced by BGNs (80 μg/mL) in the presence or absence of inhibitor SB 431542. (A) Western blotting analysis for RUNX2, OPN, SMAD3 and phosphorylated-SMAD3 (p-SMAD3) proteins expression on day 14, GAPDH is the housekeepingprotein; (B-E) Relative gray intensity of RUNX2 (B), OPN (C), SMAD3 (D), p-SMAD3 (E) proteins calculated based on western blotting patterns; (F-G)Relative expression

of osteogenic marker genes *Runx2*(F) and *Opn*(G) of ASCs after culture for 7 and 14 days.NC is the negative control.*P<0.05 and **P<0.01.

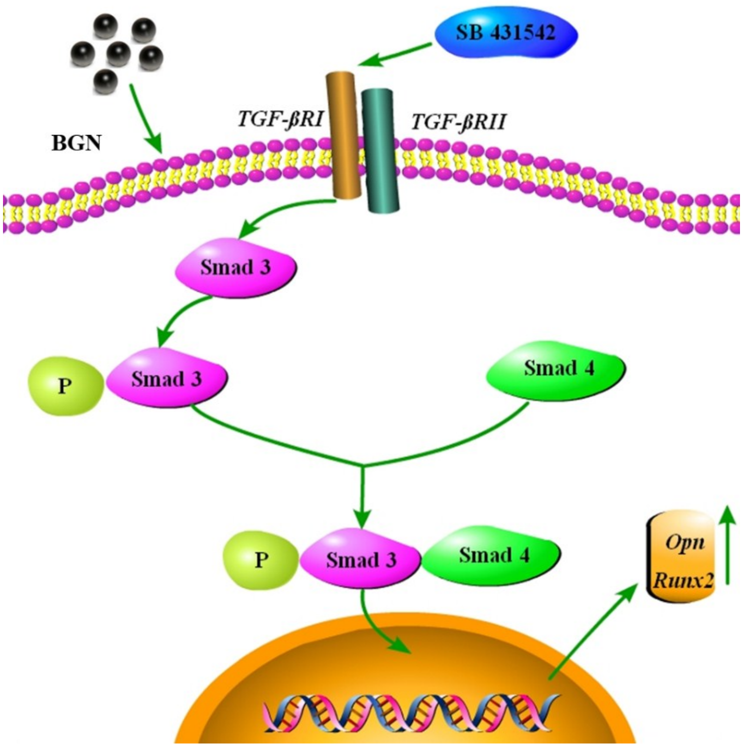

Scheme 1. Schemetic illustration showing the molecular mechanism of the modulation of osteogenic differentiation of ASCs by monodispersed BGNs through TGF-beta/Smad3 signaling pathway. SB 431542 was used as a TGF-beta/Smad3 signaling pathway inhibitor.

Table of Content Graphic

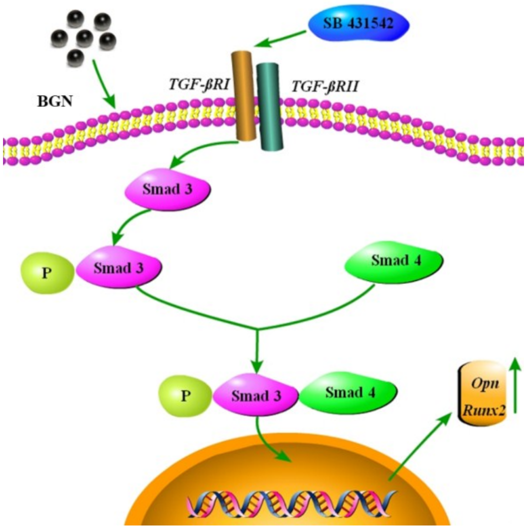

Abstract: Monodispersed bioactive glass nanoparticles (BGNs) were used to regulate the osteogenic differentiation of adipose-derived stem cells (ASCs). BGNs (100-200 nm) with 80 μg/mL could significantly enhance the osteogenic differentiation of ASCs through upregulating the ALP activity, osteogenic genes and protein expressions (Runx2 and Opn), as well as calcium deposition, through the activation of TGF-beta/Smad3 signaling pathway.